Tracking Algorithms Aided by the Pose of Target

DAI LIU[1,2], YONGBO ZHAO[1], AND BAOQING XU[1]
[1]National Laboratory of Radar Signal Processing, Xidian University, Xi'an 710071, China
[2]Xi'an Electronic Engineering Research Institute, Xi'an 710100, China

Corresponding author: Yongbo Zhao (ybzhao@xidian.edu.cn)

ABSTRACT The traditional target tracking algorithms have utilized the information on the target position. With the development of radar high-resolution technology, it is possible to obtain the pose of target. In this paper, two target tracking algorithms aided by the pose of target are proposed. First, the pose of the target is estimated in the real time by the high-resolution range profile, and then, the pose is added to the target measurement equation. Because the relationship between the pose and the motion parameters of the targets is nonlinear, the extended Kalman filter algorithm aided by the pose of target (Pose-EKF) and the unscented Kalman filter algorithm aided by the pose of target (Pose-UKF) are proposed. The results of simulation demonstrate that compared with the traditional extended Kalman filter algorithm (EKF) and the traditional Unscented Kalman filter algorithm (UKF), the proposed algorithm can greatly improve the target tracking accuracy (position precision and velocity precision) and the convergence speed. The pose measurement error has a little effect on the tracking performance. The difference in the tracking accuracy between Pose-EKF and Pose-UKF is very little. But the Pose-EKF is better than Pose-UKF in terms of computation time, but Pose-EKF fails and Pose-UKF is effective when the pose is critical.

INDEX TERMS Target tracking, pose measure, the extended Kalman filter, the unscented Kalman filter, the high resolution range profile.

I. INTRODUCTION

Target tracking algorithm is an important research topic in the field of radar data processing [1]–[4]. The traditional target tracking algorithms are based on the observations of target distance, azimuth angle and elevation angle. With the development of radar technology, Radar Cross Section (RCS) [5]–[7], radial velocity [8]–[10], target amplitude [11]–[13] and High Resolution Range Profile (HRRP) [14], [15] are acquired and applied for radar target tracking. In [5], the noncoherent pulse integration on RCS-assisted tracking can gain the potential benefit. The authors in [6] propose a RCS estimation scheme for air targets generalized to ground-moving objects and then implemented into the Gaussian mixture probability hypothesis density filter. RCS is estimated and used as additional target attribute information, which can improve the tracking performance, but the advantage of RCS-assisted tracking is limited in [7]. In [8]–[10], the radial velocity using Doppler measurements has been applied to Kalman filter to improve the target tracking performance. In [11], the new conservative amplitude likelihoods for the probabilistic data association filter with amplitude information are proposed to improve

the robustness. An expectation–maximization algorithm was proposed for Bayesian track-before-detect with target amplitude function which can improve the performance of detection and tracking in [12]. In [13], the modified Riccati equation was evaluated with amplitude information for the case of more precisely K-distributed, background noise, or a Swerling I target in heavy-tailed. In [14], the new formulation from the scattering centers high-resolution range (HRR) measurements has been developed, based on target motion features. In [15], local motion features extracted from HRRP was used to assist data association.

With the development of high resolution radar technology, the acquisition of target pose becomes a possibility [16]–[18]. In [16], the authors propose a pose estimation algorithm using HRRP which can be obtained from the high resolution radar, and the algorithm is based on motion state filtering and profile matching and applied to the missile track. In this paper, two tracking algorithms aided by the pose of target were proposed. It includes the extended Kalman filter algorithm aided by the pose of target (Pose-EKF) and the Unscented Kalman filter algorithm aided by the pose of target (Pose-UKF). Firstly, the pose of the target is estimated in

the real time by HRRP, and then the pose is added to the target measurement equation. Then because the relationship between the pose and the motion parameters of the targets is nonlinear, Pose-EKF uses the Taylor series expansion to linearize the pose, and Pose-UKF approximates the posterior probability density function (PDF) of the state vector and performs Unscented Kalman filter (UKF). Particle filter algorithm (PF) is not adopted because of its large amount of calculation and low engineering application value. In this paper, the proposed algorithms are compared with the traditional extended Kalman filter algorithm (EKF) [21]–[23] and the traditional UKF [24]–[26] in the following aspects: the root mean square error of the target position, the mean square error of the velocity, the convergence speed and the computation time. The proposed algorithms can greatly improve the target tracking accuracy (position precision and velocity precision) and the convergence speed, and the Pose-EKF is better than Pose-UKF in terms of computation time. Meanwhile the effect of the pose measurement error on the target tracking performance is analyzed, and the pose measurement error has little effect on the tracking performance.
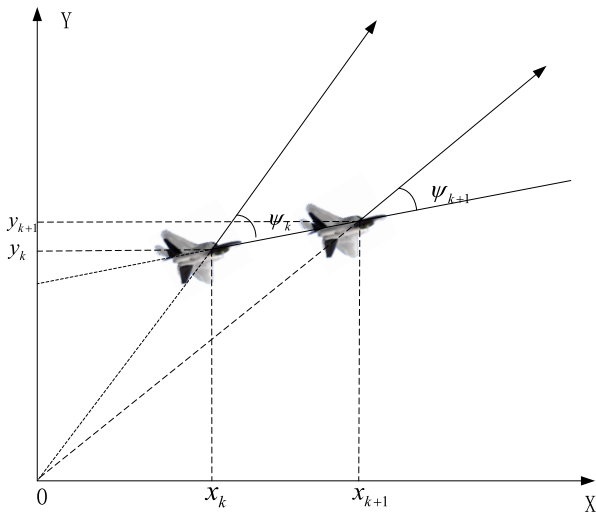

FIGURE 1. The define of the pose.

II. POSE OF TARGET

As shown in Fig. 1, the pose of target obtained by HRRP is defined as the angle between velocity vector and position vector.

$$\cos \psi = \frac{(x, y)^T \cdot (\dot{x}, \dot{y})^T}{\| (x, y)^T \| \cdot \| (\dot{x}, \dot{y})^T \|} = \frac{x\dot{x} + y\dot{y}}{\sqrt{x^2 + y^2}\sqrt{\dot{x}^2 + \dot{y}^2}} \quad (1)$$

$$\psi = \arccos(\frac{x\dot{x} + y\dot{y}}{\sqrt{x^2 + y^2}\sqrt{\dot{x}^2 + \dot{y}^2}})(0 \leq \psi \leq 180) \quad (2)$$

where (x, y) is position vector and $(\dot{x}, \dot{y})$ is velocity vector.

III. MATHEMATICAL MODE

Assume that the target moves uniformly in a straight line in $x - y - z$ plane.

The equation of the state can be described as

$$x_k = F_{k|k-1} x_{k-1} + w_{k-1} \quad (3)$$

where $x_k = [x_{Tk}, \dot{x}_{Tk}, y_{Tk}, \dot{y}_{Tk}, z_{Tk}, \dot{z}_{Tk}]^T$ denotes the motion state at time k, superscript T denotes the transpose of the matrix, (x_{Tk}, y_{Tk}, z_{Tk}) denotes the position of target, $(\dot{x}_{Tk}, \dot{y}_{Tk}, \dot{z}_{Tk})$ denotes the velocity of target, $F_{k|k-1}$ denotes the transitional matrix, w_{k-1} denotes a zero-mean Gaussian noise with state noise intensity σ_w^2 and covariance Q.

$$F_{k|k-1} = \begin{bmatrix} 1 & T & 0 & 0 & 0 & 0 \\ 0 & 1 & 0 & 0 & 0 & 0 \\ 0 & 0 & 1 & T & 0 & 0 \\ 0 & 0 & 0 & 1 & 0 & 0 \\ 0 & 0 & 0 & 0 & 1 & T \\ 0 & 0 & 0 & 0 & 0 & 1 \end{bmatrix}$$

$$Q = \sigma_w^2 \begin{bmatrix} T^3/3 & T^2/2 & 0 & 0 & 0 & 0 \\ T^2/2 & T & 0 & 0 & 0 & 0 \\ 0 & 0 & T^3/3 & T^2/2 & 0 & 0 \\ 0 & 0 & T^2/2 & T & 0 & 0 \\ 0 & 0 & 0 & 0 & T^3/3 & T^2/2 \\ 0 & 0 & 0 & 0 & T^2/2 & T \end{bmatrix}$$

The "T" in the matrix expression represents the sampling interval.

The equation of the measurement can be described as:

$$z_k = h(x_k) + v_k \quad (4)$$

where z_k denotes the measurement at time k, $z_k = [r_{Tk}, \theta_{Tk}, \varphi_{Tk}, \psi_{Tk}]^T$, r_{Tk} denotes the radial distance of target at time k, θ_{Tk} denotes the azimuth of target at time k, φ_{Tk} denotes the elevation of target at time k, ψ_{Tk} denotes the pose of target at time k, $h(\bullet)$ denotes the measurement function, and v_k denotes a zero-mean Gaussian observation noise with covariance R.

$$h(x_k) = \begin{bmatrix} \sqrt{x_k^2 + y_k^2 + z_k^2} \\ \arctan(y_k/x_k) \\ \arctan(z_k/\sqrt{x_k^2 + y_k^2}) \\ \arccos(\frac{x_k \dot{x}_k + y_k \dot{y}_k}{\sqrt{x_k^2 + y_k^2}\sqrt{\dot{x}_k^2 + \dot{y}_k^2}}) \end{bmatrix} \quad (5)$$

IV. TRACKING ALGORITHMS AIDED BY THE POSE OF TARGET

A. IMPLEMENTATION PROCESS

The implementation process of tracking algorithm aided by the pose of target is as shown in Fig. 2. Firstly, Using actual measurement or electromagnetic simulation calculation, the target range profile database is established in off-line state and normalized. According to requirements for accuracy of pose estimation, multiple angle intervals are divided, and the range profile templates of each angle interval are pre-stored. Secondly, On-line state, the radar can measure the target range profile in real time and match the range profile templates. Because of the huge amount of calculation,
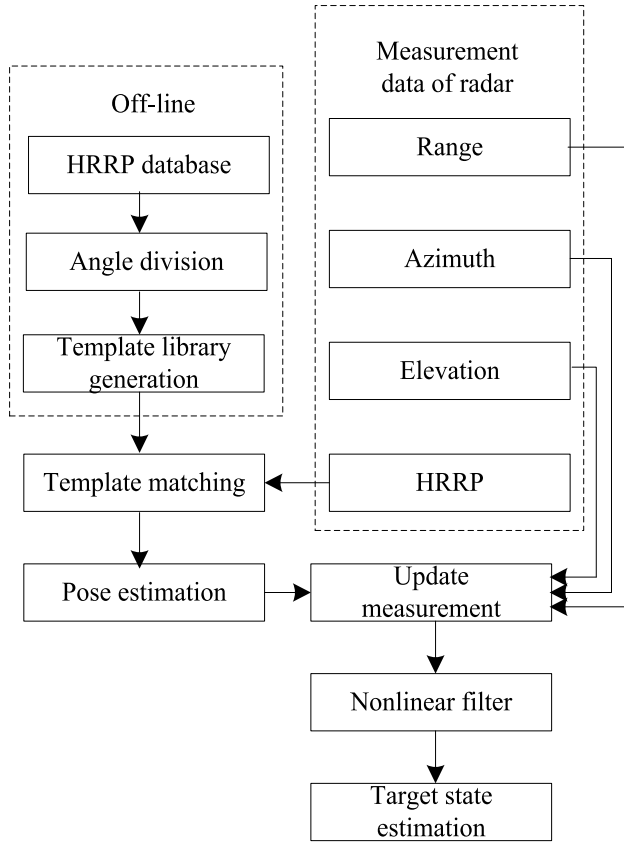
FIGURE 2. The implementation process of tracking algorithm.

the pose of target can be predicted by using the motion state information and equation (1), so that the optimal value can be searched in a small range. On the one hand, the computational cost can be reduced. On the other hand, the outliers of the pose estimation can be eliminated. According to certain recognition conditions, the pose of target can be obtained. Finally, the pose, distance, azimuth and elevation of target are added to the measurement of radar to non-linear filter and estimate the target state. In this paper, Pose-EKF algorithm is proposed by combining the pose aid with EKF algorithm, and Pose-UKF algorithm is proposed by combining the pose aid with UKF algorithm.

B. Pose_EKF ALGORITHM
1) LINEARIZING THE MEASUREMENT EQUATION
The pose in the measurement equation is a nonlinear function. The pose is linearized by carrying out the Taylor series expansion and omitting high-order quantities, and then the nonlinear problem is transformed into a linear problem.

The target measurement prediction equation is written in matrix form as follows.

$$Z_{k|k-1} = h(\hat{X}_{k|k-1}) \tag{6}$$

For $0 < \beta < 180$,

$$\frac{\partial \psi}{\partial X}\Big|_{X=\hat{X}_{k|k-1}} = \frac{\partial(\arccos(\frac{x\dot{x}+y\dot{y}}{\sqrt{x^2+y^2}\sqrt{\dot{x}^2+\dot{y}^2}}))}{\partial X}\Big|_{X=\hat{X}_{k|k-1}}$$

Let $C = \arccos(\frac{x\dot{x}+y\dot{y}}{\sqrt{x^2+y^2}\sqrt{\dot{x}^2+\dot{y}^2}})$,

$$\frac{\partial \psi}{\partial X}\Big|_{X=\hat{X}_{k|k-1}} = -\frac{1}{\sqrt{1-C^2}}\frac{\partial C}{\partial X}\Big|_{X=\hat{X}_{k|k-1}}$$

$$= -\frac{1}{\sqrt{1-C^2}}\frac{\partial(\frac{x\dot{x}+y\dot{y}}{\sqrt{x^2+y^2}\sqrt{\dot{x}^2+\dot{y}^2}})}{\partial X}\Big|_{X=\hat{X}_{k|k-1}}$$

$$= -\frac{1}{\sqrt{1-C^2}}\frac{\partial(\frac{x\dot{x}+y\dot{y}}{\sqrt{x^2+y^2}}\cdot\frac{1}{\sqrt{\dot{x}^2+\dot{y}^2}})}{\partial X}\Big|_{X=\hat{X}_{k|k-1}}$$

$$= -\frac{1}{\sqrt{1-C^2}}(\frac{1}{\sqrt{\dot{x}^2+\dot{y}^2}}\cdot\frac{\partial(\frac{x\dot{x}+y\dot{y}}{\sqrt{x^2+y^2}})}{\partial X}\Big|_{X=\hat{X}_{k|k-1}}$$

$$+ \frac{x\dot{x}+y\dot{y}}{\sqrt{x^2+y^2}}\cdot\frac{\partial(\frac{1}{\sqrt{\dot{x}^2+\dot{y}^2}})}{\partial X}\Big|_{X=\hat{X}_{k|k-1}}) \tag{7}$$

where

$$\frac{\partial(\frac{x\dot{x}+y\dot{y}}{\sqrt{x^2+y^2}})}{\partial X}\Big|_{X=\hat{X}_{k|k-1}}$$
$$= [(\hat{\dot{x}}_{k|k-1}\hat{y}^2_{k|k-1}-\hat{\dot{y}}_{k|k-1}\hat{x}_{k|k-1}\hat{y}_{k|k-1})/(\hat{x}^2_{k|k-1}+\hat{y}^2_{k|k-1})^{3/2},$$
$$\hat{x}_{k|k-1}/(\hat{x}^2_{k|k-1}+\hat{y}^2_{k|k-1})^{1/2},$$
$$(\hat{\dot{y}}_{k|k-1}\hat{x}^2_{k|k-1}-\hat{\dot{x}}_{k|k-1}\hat{x}_{k|k-1}\hat{y}_{k|k-1})/(\hat{x}^2_{k|k-1}+\hat{y}^2_{k|k-1})^{3/2},$$
$$\hat{y}_{k|k-1}/(\hat{x}^2_{k|k-1}+\hat{y}^2_{k|k-1})^{1/2}, 0, 0] \tag{8}$$

$$\frac{\partial(\frac{1}{\sqrt{\dot{x}^2+\dot{y}^2}})}{\partial X}\Big|_{X=\hat{X}_{k|k-1}}$$
$$= [0, -\hat{\dot{x}}_{k|k-1}/(\hat{\dot{x}}^2_{k|k-1}+\hat{\dot{y}}^2_{k|k-1})^{3/2}, 0,$$
$$-\hat{\dot{y}}_{k|k-1}/(\hat{\dot{x}}^2_{k|k-1}+\hat{\dot{y}}^2_{k|k-1})^{3/2}, 0, 0] \tag{9}$$

Substituting equation (8) and equation (9) into equation (7),

For $\hat{x}_{k|k-1}\hat{y}_{k|k-1} \geq \hat{x}_{k|k-1}\hat{\dot{y}}_{k|k-1}$,

$$\frac{\partial \psi}{\partial X}\Big|_{X=\hat{X}_{k|k-1}}$$
$$= [-\hat{y}_{k|k-1}/(\hat{x}^2_{k|k-1}+\hat{y}^2_{k|k-1}), \hat{\dot{y}}_{k|k-1}/(\hat{\dot{x}}^2_{k|k-1}+\hat{\dot{y}}^2_{k|k-1}),$$
$$-\hat{x}_{k|k-1}/(\hat{x}^2_{k|k-1}+\hat{y}^2_{k|k-1}), \hat{\dot{x}}_{k|k-1}/(\hat{\dot{x}}^2_{k|k-1}+\hat{\dot{y}}^2_{k|k-1}), 0, 0]$$

For $\hat{x}_{k|k-1}\hat{y}_{k|k-1} \prec \hat{x}_{k|k-1}\hat{\dot{y}}_{k|k-1}$,

$$\frac{\partial \psi}{\partial X}\Big|_{X=\hat{X}_{k|k-1}}$$
$$= [\hat{y}_{k|k-1}/(\hat{x}^2_{k|k-1}+\hat{y}^2_{k|k-1}), -\hat{\dot{y}}_{k|k-1}/(\hat{\dot{x}}^2_{k|k-1}+\hat{\dot{y}}^2_{k|k-1}),$$
$$\hat{x}_{k|k-1}/(\hat{x}^2_{k|k-1}+\hat{y}^2_{k|k-1}), -\hat{\dot{x}}_{k|k-1}/(\hat{\dot{x}}^2_{k|k-1}+\hat{\dot{y}}^2_{k|k-1}), 0, 0]$$

The measurement matrix $H(k)$ is as follows:

$$H(k) = \frac{\partial h}{\partial X}\Big|_{X=\hat{X}_{k|k-1}}$$

$$= \begin{bmatrix} H_{11} & H_{12} & H_{13} & H_{14} & H_{15} & H_{16} \\ H_{21} & H_{22} & H_{23} & H_{24} & H_{25} & H_{26} \\ H_{31} & H_{32} & H_{33} & H_{34} & H_{35} & H_{36} \\ H_{41} & H_{42} & H_{43} & H_{44} & H_{45} & H_{46} \end{bmatrix}$$

$$H_{11} = \hat{x}_{k|k-1}/(\hat{x}^2_{k|k-1}+\hat{y}^2_{k|k-1}+\hat{z}^2_{k|k-1})^{1/2}$$

$$H_{13} = \hat{y}_{k|k-1}/(\hat{x}^2_{k|k-1} + \hat{y}^2_{k|k-1} + \hat{z}^2_{k|k-1})^{1/2}$$

$$H_{15} = \hat{z}_{k|k-1}/(\hat{x}^2_{k|k-1} + \hat{y}^2_{k|k-1} + \hat{z}^2_{k|k-1})^{1/2}$$

$$H_{21} = -\hat{y}_{k|k-1}/(\hat{x}^2_{k|k-1} + \hat{y}^2_{k|k-1})^{1/2}$$

$$H_{23} = \hat{x}_{k|k-1}/(\hat{x}^2_{k|k-1} + \hat{y}^2_{k|k-1})^{1/2}$$

$$H_{31} = -\hat{x}_{k-1}\hat{z}_{k|k-1}/[(\hat{x}^2_{k|k-1} + \hat{y}^2_{k|k-1})^{1/2}$$
$$\times (\hat{x}^2_{k|k-1} + \hat{y}^2_{k|k-1} + \hat{z}^2_{k|k-1})]$$

$$H_{33} = -\hat{y}_{k|k-1}\hat{z}_{k|k-1}/[(\hat{x}^2_{k|k-1} + \hat{y}^2_{k|k-1})^{1/2}$$
$$\times (\hat{x}^2_{k|k-1} + \hat{y}^2_{k|k-1} + \hat{z}^2_{k|k-1})]$$

$$H_{35} = (\hat{x}^2_{k|k-1} + \hat{y}^2_{k|k-1})^{1/2}/(\hat{x}^2_{k|k-1} + \hat{y}^2_{k|k-1} + \hat{z}^2_{k|k-1})$$

$$H_{41} = \begin{cases} -\hat{y}_{k|k-1}/(\hat{x}^2_{k|k-1} + \hat{y}^2_{k|k-1}) \\ \qquad \hat{x}_{k|k-1}\hat{y}_{k|k-1} \geq \hat{x}_{k|k-1}\hat{y}_{k|k-1} \\ \hat{y}_{k|k-1}/(\hat{x}^2_{k|k-1} + \hat{y}^2_{k|k-1}) \\ \qquad \hat{x}_{k|k-1}\hat{y}_{k|k-1} \prec \hat{x}_{k|k-1}\hat{y}_{k|k-1} \end{cases}$$

$$H_{42} = \begin{cases} \hat{y}_{k|k-1}/(\hat{x}^2_{k|k-1} + \hat{y}^2_{k|k-1}) \\ \qquad \hat{x}_{k|k-1}\hat{y}_{k|k-1} \geq \hat{x}_{k|k-1}\hat{y}_{k|k-1} \\ -\hat{y}_{k|k-1}/(\hat{x}^2_{k|k-1} + \hat{y}^2_{k|k-1}) \\ \qquad \hat{x}_{k|k-1}\hat{y}_{k|k-1} \prec \hat{x}_{k|k-1}\hat{y}_{k|k-1} \end{cases}$$

$$H_{43} = \begin{cases} -\hat{x}_{k|k-1}/(\hat{x}^2_{k|k-1} + \hat{y}^2_{k|k-1}) \\ \qquad \hat{x}_{k|k-1}\hat{y}_{k|k-1} \geq \hat{x}_{k|k-1}\hat{y}_{k|k-1} \\ \hat{x}_{k|k-1}/(\hat{x}^2_{k|k-1} + \hat{y}^2_{k|k-1}) \\ \qquad \hat{x}_{k|k-1}\hat{y}_{k|k-1} \prec \hat{x}_{k|k-1}\hat{y}_{k|k-1} \end{cases}$$

$$H_{44} = \begin{cases} \hat{x}_{k|k-1}/(\hat{x}^2_{k|k-1} + \hat{y}^2_{k|k-1}) \\ \qquad \hat{x}_{k|k-1}\hat{y}_{k|k-1} \geq \hat{x}_{k|k-1}\hat{y}_{k|k-1} \\ -\hat{x}_{k|k-1}/(\hat{x}^2_{k|k-1} + \hat{y}^2_{k|k-1}) \\ \qquad \hat{x}_{k|k-1}\hat{y}_{k|k-1} \prec \hat{x}_{k|k-1}\hat{y}_{k|k-1} \end{cases}$$

$$H_{12} = 0, \quad H_{14} = 0, \quad H_{16} = 0, \quad H_{22} = 0,$$
$$H_{24} = 0, H_{26} = 0, \quad H_{32} = 0, \quad H_{34} = 0,$$
$$H_{36} = 0, \quad H_{45} = 0, \quad H_{46} = 0 \tag{10}$$

2) Pose_EKF ALGORITHM

Suppose that the target state is $\hat{X}_{k-1|k-1}$, the covariance matrix is $P_{k-1|k-1}$ at time k-1, and the measurement at time k is z_k. $z_k = [r_{Tk}, \theta_{Tk}, \varphi_{Tk}, \psi_{Tk}]^T$. The detailed steps of the Pose_EKF algorithm aided by the pose of target are as follows:

Step 1: predict the target state at time k.

$$\hat{X}_{k|k-1} = F\hat{X}_{k-1|k-1} \tag{11}$$

Step 2: predict the covariance matrix at time k.

$$P_{k|k-1} = FP_{k-1|k-1}F^T + Q_{k-1} \tag{12}$$

Step 3: calculate the Kalman gain

$$K_k = P_{k|k-1}H_kS_k^1 \tag{13}$$

where H_k is the Jacobian matrix of the measurement function, and S_k is the measurement prediction covariance.

$$H_k = (\Delta_{x_k}h^T(X_k))^T \tag{14}$$

$$S_k = H_kP_{k|k-1}H_k^T + R_k \tag{15}$$

Step 4: the pose of target ψ_{Tk} obtained by HRRP is used to form the measurement $z_k = [r_{Tk}, \theta_{Tk}, \varphi_{Tk}, \psi_{Tk}]^T$.

Step 5: update the target state at time k.

$$\hat{X}_{k|k} = \hat{X}_{k|k-1} + K_k(z_k - h(\hat{X}_{k|k-1})) \tag{16}$$

Step 6: update the covariance matrix at time k.

$$P_{k|k} = [I - K_kH_k]P_{k|k-1}[I - K_kH_k]^T - K_kR_kK_k^T \tag{17}$$

The shortage of this algorithm is $\psi_{Tk} \neq 0$ and $\psi_{Tk} \neq 180$. In other words, Pose-EKF fails when the pose is critical.

C. Pose_UKF ALGORITHM

UKF does not need to linearize the measurement equation, but approximates the posterior probability density function (PDF) of the state vector, and then performs recursive filtering in the framework of standard Kalman filter. The Pose-UKF algorithm adds the pose of target to the equation of measurement and performs UKF. The detailed steps of the Pose_UKF algorithm aided by the pose of target are as follows:

Step 1: Parameters Initialization.

$$\hat{x}_{0|0} = E(x_0) \tag{18}$$

$$P_{0|0} = E((x_0 - \hat{x}_{0|0})(x_0 - \hat{x}_{0|0})^T) \tag{19}$$

where x_0 denotes the initial state vector, $\hat{x}_{0|0}$ denotes the estimated value of initial state vector, $P_{0|0}$ denotes the estimated value of the initial error covariance matrix.

Step 2: Time Update

$$\begin{cases} \chi^0_{k-1|k-1} = \hat{x}_{k-1|k-1} \\ \chi^i_{k-1|k-1} = \hat{x}_{k-1|k-1} + (\sqrt{(n+\lambda)P_{k-1|k-1}}), \\ \qquad\qquad\qquad i = 1, 2, ..., n \\ \chi^i_{k-1|k-1} = \hat{x}_{k-1|k-1} - (\sqrt{(n+\lambda)P_{k-1|k-1}}), \\ \qquad\qquad\qquad i = n+1, n+2, ..., 2n \end{cases} \tag{20}$$

$$\begin{cases} \omega^m_0 = \kappa/(n+\kappa) \\ \omega^c_0 = \kappa/(n+\kappa) + 1 - \alpha^2 + \gamma \\ \omega^m_i = \omega^c_i = \kappa/[2(n+\kappa)], \qquad i = 1, ..., 2n \end{cases} \tag{21}$$

$$\chi^i_{k|k-1} = F \cdot \chi^i_{k-1|k-1} \tag{22}$$

Predict the target state at time k:

$$\hat{x}_{k|k-1} = F\hat{x}_{k-1|k-1} \tag{23}$$

Predict the covariance matrix at time k:

$$P_{k|k-1} = \sum_{i=0}^{2n} \omega^c_i (\chi^i_{k|k-1} - \hat{x}_{k|k-1})(\chi^i_{k|k-1} - \hat{x}_{k|k-1})^T + Q_{k-1} \tag{24}$$

where ω^c_i is the weight used to calculate the estimated mean of $\chi^i_{k-1|k-1}$, ω^m_i is the weight used to calculate the estimated covariance matrix of $\chi^i_{k-1|k-1}$.

Step 3: Measurement Update.

The pose of target ψ_{Tk} obtained by HRRP is used to form the measurement $z_k = [r_{Tk}, \theta_{Tk}, \varphi_{Tk}, \psi_{Tk}]^T$.

$$\xi_{k|k-1}^i = h(\chi_{k|k-1}^i) \tag{25}$$

$$\hat{z}_{k|k-1} = \sum_{i=0}^{2n} \omega_i^m \xi_{k|k-1}^i \tag{26}$$

$$P_{z_k} = \sum_{i=0}^{2n} \omega_i^c (\xi_{k|k-1}^i - \hat{z}_{k|k-1}) \cdot (\xi_{k|k-1}^i - \hat{z}_{k|k-1})^T \tag{27}$$

$$P_{x_k z_k} = \sum_{i=0}^{2n} \omega_i^c (\chi_{k|k-1}^i - \hat{x}_{k|k-1}) \cdot (\xi_{k|k-1}^i - \hat{z}_{k|k-1})^T \tag{28}$$

Step 4: Filter Update

Calculate the Kalman gain:

$$K_k = P_{z_k} P_{x_k z_k}^{-1} \tag{29}$$

Update the target state at time k:

$$\hat{x}_{k|k} = \hat{x}_{k|k-1} + K_k(z_k - \hat{z}_{k|k-1}) \tag{30}$$

Update the covariance matrix at time k:

$$P_{k|k} = P_{k|k-1} - K_k P_{z_k} K_k^T \tag{31}$$

The advantage of the Pose-UKF algorithm relative to the Pose-EKF algorithm is that the Pose-UKF algorithm is effective when the pose is critical. The performance of the two algorithms will be compared in the following simulation.

V. SIMULATIONS AND ANALYSIS

In order to illustrate the performance of the proposed algorithms, the following scenario has been designed A target is assumed to fly out of its initial position (12000m, 12000m, 1000m), the X-axis velocity is 100m/s, and the Y-axis velocity is - 80m/s in a uniform linear motion. The altitude remains unchanged at 1000m. The trajectory of the target for a single run is sh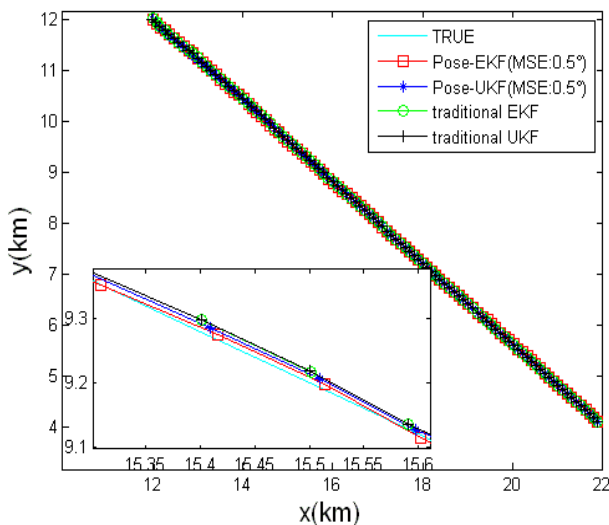own in Fig. 3. The data are observed every 1s and the simulation lasts 100s. In the simulation, the error of measuring distance is 30m, the error of measuring azimuth is 0.06°. HRRP template matching method is used to estimate the pose the target. According to the range of pose, 3600 angle intervals are divided, and the range profile templates of each angle interval are pre-stored. Radar can measure the target range profile in real time and match the range profile templates, and the pose of target can be obtained. The pose interval of the target range profile database is 0.1°, and the error of measuring pose are 0.5° and 1° respectively. The 200 Monte Carlo simulations have been done. The process noise is white noise whose mean value is 0 and variance is 1. Pose-EKF algorithm, Pose-UKF algorithm, traditional EKF algorithm and traditional UKF algorithm are used to compare respectively.

The root mean square error (RMSE) of target position is defined as

$$RMSE_{pk} = \sqrt{\frac{1}{N} \sum_{i=1}^{N} [(x_{Tk} - x_{Tk}^i)^2 + (y_{Tk} - y_{Tk}^i)^2]} \tag{32}$$

The root mean square error of target velocity is defined as

$$RMSE_{vk} = \sqrt{\frac{1}{N} \sum_{i=1}^{N} [(\dot{x}_{Tk} - \dot{x}_{Tk}^i)^2 + (\dot{y}_{Tk} - \dot{y}_{Tk}^i)^2]} \tag{33}$$

where N is the number of Monte Carlo experiments, (x_{Tk}^i, y_{Tk}^i) is the target position, and $(\dot{x}_{Tk}^i, \dot{y}_{Tk}^i)$ is the target velocity estimated in the i experiment at time k.

The Pose-EKF algorithm and the Pose-UKF algorithm proposed in this paper are compared with the traditional EKF algorithm and the traditional UKF algorithm. The results are compared from four aspects: the root mean square error of the target position, the mean square error of the velocity, the convergence speed and the computation time.
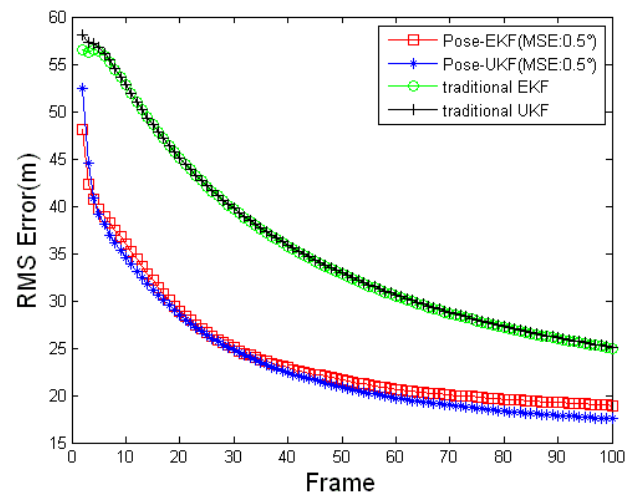
FIGURE 3. The trajectory of the target for a single run.

FIGURE 4. RMSE of target position.

From the RMSE curve of target position in Fig. 4, it can be seen that the RMSE of target position of the traditional

EKF algorithm and the traditional UKF algorithm is 25 m, while adopting our proposed algorithm, the RMSE of target position of the Pose-EKF algorithm is 19 m and that of the Pose-UKF algorithm is 18 m when the error of measuring pose is 0.5°. The Pose-UKF algorithm is almost the same as the Pose-EKF algorithm in the accuracy of target position, and has higher precision than the traditional EKF algorithm and the traditional UKF algorithm. From the convergence speed of target position error, The Pose-UKF algorithm and the Pose-EKF algorithm are also faster than the traditional EKF algorithm and the traditional UKF algorithm.
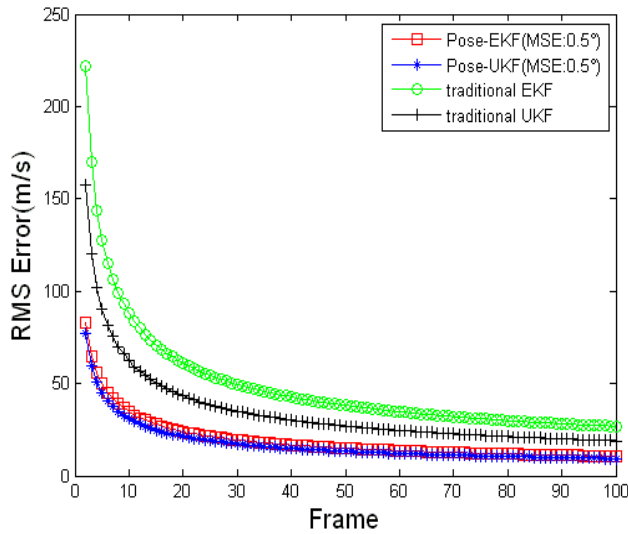

FIGURE 5. RMSE of target velocity.

From the RMSE curve of target velocity in Fig. 5, it can be seen that the RMSE of target velocity of the traditional EKF algorithm is 27 m/s, and that of the traditional UKF algorithm is 19 m/s, while adopting our proposed algorithm, the RMSE of target velocity of the Pose-EKF algorithm and the Pose-UKF algorithm is 9 m/s. The Pose-UKF algorithm is almost the same as the Pose-EKF algorithm in the accuracy of target velocity. The Pose-UKF algorithm and the Pose-EKF algorithm are higher in the accuracy of target velocity, and faster in the convergence speed of target velocity error than the traditional EKF algorithm and the traditional UKF algorithm.

From the computation time curve in Fig. 6, it can be seen that the traditional EKF algorithm takes 50 us to compute, the traditional UKF algorithm takes 156 us to compute, the Pose-EKF algorithm takes 64 us to compute, and the Pose-UKF algorithm takes 165 us to compute. The traditional EKF algorithm is the best in the computation time, followed by the Pose-EKF algorithm, and then the traditional UKF algorithm and the Pose-UKF algorithm. Because the pose is added to the target observation, the Pose-EKF algorithm is more time-consuming than the traditional EKF algorithm, and the Pose-UKF algorithm is more time-consuming than the traditional UKF algorithm. Comparing the Pose-EKF algorithm with the Pose-UKF algorithm, the Pose-EKF
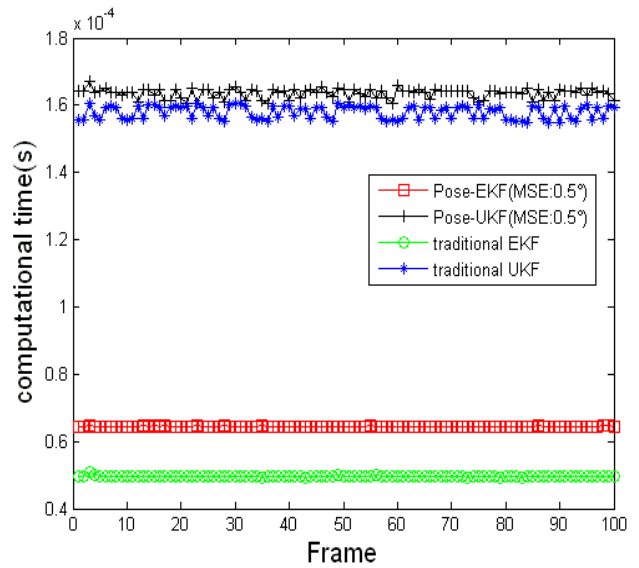

FIGURE 6. The computational time of four algorithms.

algorithm is better than the Pose-UKF algorithm in terms of computation time.
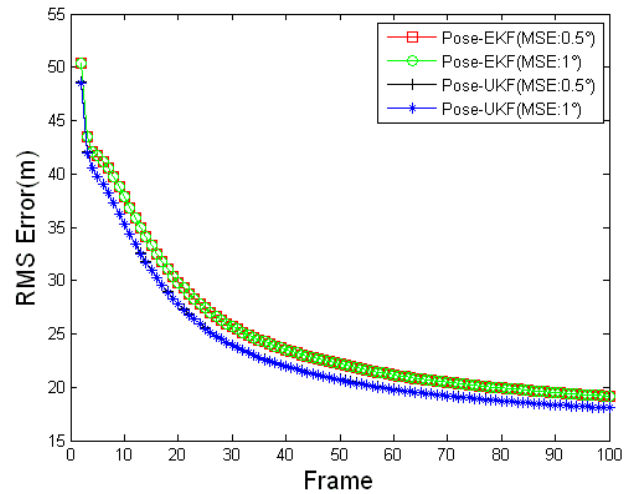

FIGURE 7. RMSE of target position varied with different pose error.

The effect of pose error on the performance of Pose-EKF algorithm and Pose-UKF algorithm has been also analyzed. As can be seen from Fig. 7 and Fig. 8, when the pose error is 2 times of the pose accuracy, the RMSE of the target position of Pose-EKF algorithm is 19 m, RMSE of the target velocity of Pose-EKF algorithm is 10 m/s, the RMSE of the target position of Pose-UKF algorithm is 18 m, and the RMSE of the target velocity of Pose-UKF algorithm is 10 m/s. The error of pose has little effect on the performance of Pose-EKF algorithm and Pose-UKF algorithm, and it can be neglected.

As mentioned above, Pose-EKF algorithm and Pose-UKF algorithm are superior to the traditional EKF algorithm and UKF algorithm in performance, embodied in the fast convergence speed, small the RMSE of the target position, small RMSE of the target velocity In terms of computation time, the Pose-EKF algorithm is superior to the
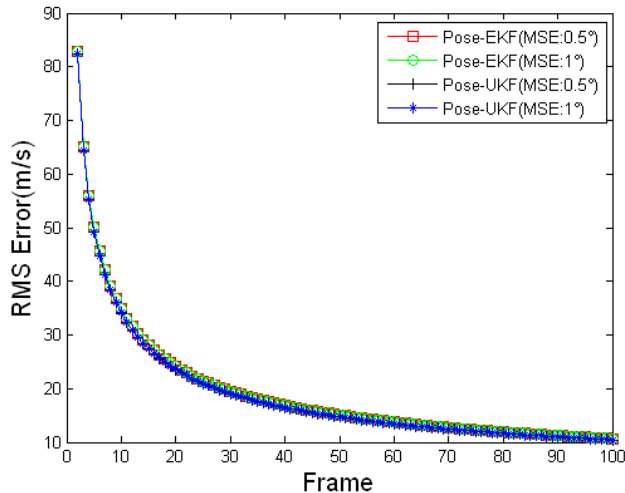
FIGURE 8. RMSE of target velocity varied with different pose error.

Pose-UKF algorithm. When the pose error does not change significantly, the performance of Pose-EKF algorithm and Pose-UKF algorithm has little effect.

VI. CONCLUSION

Compared with the traditional EKF algorithm and the traditional UKF algorithm, the proposed algorithms aided by the pose of target can improve the target tracking performance greatly. The Specific performance is reflected in the smaller RMSE of target position, the smaller RMSE of velocity and the faster convergence speed. The impact on tracking performance of pose error is little.

REFERENCES

[1] K. Granström, U. Orguner, R. Mahler, and C. Lundquist, "Corrections on: 'Extended target tracking using a Gaussian-mixture PHD filter,'" *IEEE Trans. Aerosp. Electron. Syst.*, vol. 53, no. 2, pp. 1055–1058, Apr. 2017.

[2] R. Gui, W.-Q. Wang, Y. Pan, and J. Xu, "Cognitive target tracking via angle-range-Doppler estimation with transmit subaperturing FDA radar," *IEEE J. Sel. Topics Signal Process.*, vol. 12, no. 1, pp. 76–89, Feb. 2018.

[3] D. Henke, E. M. Dominguez, D. Small, M. E. Schaepman, and E. Meier, "Moving target tracking in SAR data using combined exo- and endo-clutter processing," *IEEE Trans. Geosci. Remote Sens.*, vol. 56, no. 1, pp. 251–263, Jan. 2018.

[4] J. Yan, H. Liu, W. Pu, and Z. Bao, "Decentralized 3-D target tracking in asynchronous 2-D radar network: Algorithm and performance evaluation," *IEEE Sensors J.*, vol. 17, no. 3, pp. 823–833, Feb. 2017.

[5] L. M. Ehrman and P. R. Mahapatra, "Impact of noncoherent pulse integration on RCS-assisted tracking," *IEEE Trans. Aerosp. Electron. Syst.*, vol. 45, no. 4, pp. 1573–1579, Oct. 2009.

[6] M. Mertens, M. Ulmke, and W. Koch, "Ground target tracking with RCS estimation based on signal strength measurements," *IEEE Trans. Aerosp. Electron. Syst.*, vol. 52, no. 1, pp. 205–220, Feb. 2016.

[7] L. M. Ehrman and W. D. Blair, "Using target RCS when tracking multiple Rayleigh targets," *IEEE Trans. Aerosp. Electron. Syst.*, vol. 46, no. 2, pp. 701–716, Apr. 2010.

[8] G. Zhou, M. Pelletier, T. Kirubarajan, and T. Quan, "Statically fused converted position and Doppler measurement Kalman filters," *IEEE Trans. Aerosp. Electron. Syst.*, vol. 50, no. 1, pp. 300–318, Jan. 2014.

[9] G. Zhou, L. Wu, J. Xie, W. Deng, and T. Quan, "Constant turn model for statically fused converted measurement Kalman filters," *Signal Process.*, vol. 108, pp. 400–411, Mar. 2015.

[10] I. Klein and I. Rusnak, "Analytic solution of ECV filter with position and velocity measurements," *IEEE Trans. Aerosp. Electron. Syst.*, vol. 48, no. 2, pp. 1682–1686, Apr. 2012.

[11] E. Brekke, O. Hallingstad, and J. Glattetre, "Tracking small targets in heavy-tailed clutter using amplitude information," *IEEE J. Ocean. Eng.*, vol. 35, no. 2, pp. 314–329, Apr. 2010.

[12] S. Z. Xia and H. W. Liu, "Bayesian track-before-detect algorithm with target amplitude fluctuation based on expectation-maximisation estimation," *IET Radar, Sonar Navigat.*, vol. 6, no. 8, pp. 719–728, Oct. 2012.

[13] E. Brekke, O. Hallingstad, and J. Glattetre, "The modified riccati equation for amplitude-aided target tracking in heavy-tailed clutter," *IEEE Trans. Aerosp. Electron. Syst.*, vol. 47, no. 4, pp. 2874–2886, Oct. 2011.

[14] B. Yanxian, W. Shaoming, and W. Jun, "3D reconstruction of high-speed moving targets based on HRR measurements," *IET Radar, Sonar Navigat.*, vol. 11, no. 5, pp. 778–787, May 2017.

[15] L. Hong, N. Cui, M. Pronobis, and S. Scott, "Local motion feature aided ground moving target tracking with GMTI and HRR measurements," *IEEE Trans. Autom. Control*, vol. 50, no. 1, pp. 127–133, Jan. 2005.

[16] F. Jian-Peng, F. Hongqi, and L. Zai-Qi, "Pose estimation algorithm based on high range resolution profile," *Syst. Eng. Electron.*, vol. 34, no. 12, pp. 2413–2417, 2012.

[17] R. Opromolla, G. Fasano, G. Rufino, and M. Grassi, "Pose estimation for spacecraft relative navigation using model-based algorithms," *IEEE Trans. Aerosp. Electron. Syst.*, vol. 53, no. 1, pp. 431–447, Feb. 2017.

[18] J. Peng, W. Xu, and H. Yuan, "An efficient pose measurement method of a space non-cooperative target based on stereo vision," *IEEE Access*, vol. 5, pp. 22344–22362, 2017.

[19] H. Guo, H. Chen, F. Xu, F. Wang, and G. Lu, "Implementation of EKF for vehicle velocities estimation on FPGA," *IEEE Trans. Ind. Electron.*, vol. 60, no. 9, pp. 3823–3835, Sep. 2013.

[20] C. H. Kang, S. Y. Kim, and C. G. Park, "Adaptive complex-EKF-based DOA estimation for GPS spoofing detection," *IET Signal Process.*, vol. 12, no. 2, pp. 174–181, Apr. 2018.

[21] E. Zerdali and M. Barut, "The comparisons of optimized extended Kalman filters for speed-sensorless control of induction motors," *IEEE Trans. Ind. Electron.*, vol. 64, no. 6, pp. 4340–4351, Jun. 2017.

[22] X. Ning, F. Wang, and J. Fang, "An implicit UKF for satellite stellar refraction navigation system," *IEEE Trans. Aerosp. Electron. Syst.*, vol. 53, no. 3, pp. 1489–1503, Jun. 2017.

[23] M. Zarei-Jalalabadi and S. M.-B. Malaek, "Modification of unscented Kalman filter using a set of scaling parameters," *IET Signal Process.*, vol. 12, no. 4, pp. 471–480, Jun. 2018.

[24] H. M. T. Menegaz, J. Y. Ishihara, G. A. Borges, and A. N. Vargas, "A systematization of the unscented Kalman filter theory," *IEEE Trans. Autom. Control*, vol. 60, no. 10, pp. 2583–2598, Oct. 2015.

DAI LIU received the B.S. degree from Shandong University, Jinan, China, in 2006, and the M.E. degree from Xi'an Electronic Engineering Research Institute, Xi'an, China, in 2009.

He is currently pursuing the Ph.D. degree with the Department of Electrical Engineering, Xidian University. His research interests include radar data processing and signal processing.

YONGBO ZHAO was born in Xinxiang, Henan, China. He received the M.E. and Ph.D. degrees in electrical engineering from Xidian University, Xi'an, China, in 1997 and 2000, respectively.

He is currently a Professor with the National Laboratory of Radar Signal Processing, Xidian University. His research interests include adaptive signal processing, array signal processing, MIMO radar, and advanced radar concepts.

BAOQING XU received the B.S. degree from Qingdao Technological University, Qingdao, China, in 2014.

He is currently pursuing the Ph.D. degree with the Department of Electrical Engineering, Xidian University. His research interests include parameter estimation and adaptive signal processing.

• • •